

# Bird population trend analyses for a monitoring scheme with a highly structured sampling design

Mirjam R. Rieger<sup>1</sup>, Christoph Grüneberg<sup>2</sup>, Michael Oberhaus<sup>2</sup>, Sven Trautmann<sup>3</sup>, Madalin Parepa<sup>1</sup>, Nils Anthes<sup>1</sup>

<sup>1</sup> Institute of Evolution and Ecology, University of Tübingen, Auf der Morgenstelle 28, 72076 Tübingen, Germany

<sup>2</sup> State Agency for Nature, Environment and Consumer Protection in North Rhine-Westphalia (LANUV), 40208 Düsseldorf

<sup>3</sup> Dachverband Deutscher Avifaunisten e.V., An den Speichern 2, 48157 Münster

[nils.anthes@uni-tuebingen.de](mailto:nils.anthes@uni-tuebingen.de) (corresponding author)

## Summary

Population trends derived from systematic monitoring programmes are essential to identify species of conservation concern and to evaluate conservation measures. However, monitoring data pose several challenges for statistical analysis, including spatial bias due to an unbalanced sampling of landscapes or habitats, variation in observer expertise, frequent observer changes, and overdispersion or zero-inflation in the raw data. An additional challenge arises from so-called ‘rolling’ survey designs, where each site is only visited once within each multi-year rotation cycle. We developed a GAMM-based workflow that addresses these challenges and exemplify its application with the highly structured data from the Ecological Area Sampling (EAS) in the German federal state North-Rhine Westphalia (NRW). First, we derive a routine that allows informed decisions about the most appropriate combination of distribution family (Poisson or negative binomial), model covariates (e.g., habitat characteristics), and zero-inflation formulations to reflect species-specific data distributions. Second, we develop a correction factor that buffers population trend estimates for variation in observer expertise as reflected in variation in total bird abundance. Third, we integrate landscape-specific trends that adjust for between-year variation in the representation of habitat or landscape types within the yearly subset of sampled sites. In a consistency check, we found good match between our GAMM-based EAS trends and TRIM-based trends from the standard German common Bird monitoring scheme. The study provides a template script for *R* statistical software so the workflow can be adapted to other monitoring programmes with comparable survey designs and data structures.

*Keywords: breeding bird monitoring, trend analysis, rolling surveys, spatial bias, observer effects*

Deleted: Analysing bird

Deleted: trends from

Deleted: data

Deleted: designs

Deleted:

Deleted: model weights

## 1 Introduction

Bird populations decline worldwide (Klvaňová et al. 2009, Sauer et al. 2017, Burns et al. 2021a, Burns et al. 2021b), with the European Union alone facing an approximate loss of 560–620 million bird individuals (17–19%) within 40 years (Burns et al. 2021a, Burns et al. 2021b). Such knowledge of population sizes and their trends heavily relies on standardized monitoring programmes to provide reliable population density estimates. The resultant population trend estimates allow allocating conservation resources to species of highest conservation concern (Niemelä 2000, Buckland and Johnston 2017), provide feedback on the efficiency of conservation efforts (Johnston et al. 2015), and raise awareness for the value and state of biodiversity among decision makers and the public (Jennings 2021).

However, many monitoring programmes pose substantial challenges for statistical inference that can reduce the reliability and robustness of the estimated trends if not treated with care (Buckland and Johnston 2017). Our study focuses on a monitoring scheme with a rolling (or ‘rotating’) survey design that generates multi-year intervals between repetitive surveys per site (Buckland and Johnston 2017). Rolling surveys can cover more study sites and thus a wider range of landscape types across years than monitoring schemes with a yearly coverage of all sites but result in a large fraction of sites with missing values each year and frequent observer changes. In this context, we develop an analytical protocol to cover three core aspects. First, rolling monitoring programmes rest on spatially structured sampling designs, often coupled with between-year variation in the representation of habitat types, which needs integration into the analysis (van Strien et al. 2004, Buckland and Johnston 2017). Spatial bias arises when relevant landscape types or habitats are not represented according to their spatial coverage in the monitoring sample (van Strien et al. 2004). As a result, when population trends vary between landscapes or habitats, the estimated overall population trend can be biased towards overrepresented landscapes, or reflect changes in sample composition rather than a true change in abundance (Buckland and Johnston 2017, Bowler et al. 2022).

Second, detection probabilities and survey quality can vary strongly among and (over time) within observers, potentially introducing random and systematic trend estimation errors when ignored (Sauer et al. 1994, Link and Sauer 1998, Kéry et al. 2005, Jiguet 2009, Farmer et al. 2014). When average observer expertise remains constant, between-observer variation primarily increases (random) variation in abundance estimates between sites and years. (Sauer et al. 1994, Johnston et al. 2018). In contrast, within-observer learning and systematic changes in average observer expertise introduce (systematic) biases in trend estimates. For example, initial familiarization with a new study site and the specificities of the monitoring programme usually cause underestimated bird abundances in early survey years (Link and Sauer 1998, Jiguet 2009). Moreover, observer expertise usually increases with time after active engagement in bird territory surveys, while species detectability declines with age if

**Deleted:** existing

**Deleted:** unbiased

**Deleted:** analyses and

**Deleted:** ¶

Analytical challenges typically arise from two prime sources. First, the structure and implementation of a given monitoring programme may (i) require analytical tools for hierarchical or non-representative sampling designs

**Deleted:** , (ii) introduce random and systematic estimation errors due to variation in experience within and among observers (Sauer et al. 1994, Link and Sauer 1998, Jiguet 2009, Farmer et al. 2014), and (iii) provide small sample sizes (Svensson 1978, Nielsen et al. 2009). Second, count data such as the number of bird territories typically require consideration of (iv) properties of the underlying data distribution (Blasco-Moreno et al. 2019, Campbell 2021), (v) temporal (= serial) and spatial autocorrelation among measurements (van Strien et al. 2004, Korner-Nievergelt et al. 2015, Kéry and Royle 2020), and (vi) imperfect detection of existing territories (Kéry et al. 2005, Kéry and Royle 2020). ¶ This work focuses on three of these aspects: spatial bias due to non-representative sampling designs, observer effects and specificities of data distributions. First, spatial

**Deleted:** of the investigated region

**Deleted:** Second, the quality of trend estimates can vary with the observer (Johnston et al. 2018). Between-observer variation in expertise or other qualifications that affect survey results primarily increase (random) variation between sites and years, as long as average observer qualification remains constant...

**Deleted:** Within

**Deleted:** effects, instead, can

**Deleted:** The required

**Deleted:** any

**Deleted:** initial

**Deleted:** the

**Deleted:** since

hearing impairment reduces the detection of high-pitch bird vocalisations (Farmer et al. 2014). In rolling survey design, these general issues typically go along with a high turnover in observer identities between successive surveys of the same site, which adds further variation.

Finally, count response data as typical for bird census require models to reflect distribution properties such as overdispersion or zero inflation (Blasco-Moreno et al. 2019, Campbell 2021). Overdispersion arises when the variance of count data exceeds their mean value. It is typically resolved by modelling trends with a negative binomial error distribution instead of a Poisson distribution (Blasco-Moreno et al. 2019, Campbell 2021). Zero-inflation occurs when datasets contain so-called structural zeros. This implies a disproportionately large fraction of unoccupied sites that cannot be explained solely by sampling variation among sites considered suitable, but rather arises from survey sites that are unsuitable. Where present, structural zeros are modelled separately from the count distribution in zero-inflated model components (Korner-Nievergelt et al. 2015, Blasco-Moreno et al. 2019, Campbell 2021, Tirozzi et al. 2021).

The software TRIM (Pannekoek and van Strien 2001) represents a common analytical tool for the analysis of monitoring data and is used, for example, in the Pan European Common Bird Monitoring Scheme (Vorisek et al. 2008) and the national bird monitoring programmes of Sweden (Jiguet et al. 2013), Finland (Pöysä et al. 2013), or Germany (Kamp et al. 2021). TRIM computes trends and annual population indices from loglinear Poisson regressions. It corrects for overdispersion, serial correlation and missing values (van Strien et al. 2004) and allows weights to account for spatial bias (van Strien et al. 2004). Yet, designed for monitoring schemes with almost yearly surveys per site by the same observer, TRIM estimates are considered robust unless the turnover in survey sites between years leads to a ≥ 60 % fraction of missing values (van Strien et al. 2001, Bogaart et al. 2020, Dakki et al. 2021). Moreover, TRIM is restricted to categorical covariates, requiring climate or landscape composition covariates to be transformed into categories (Bogaart et al. 2020). Finally, long-term trend analyses beyond yearly index estimates are restricted to linear trends and breakpoint analyses, while more recent developments favour the integration of trend smoothers, e.g. with general additive (mixed) models (GA(M)Ms) (e.g., Fewster et al. (2000), Knappe (2016)). Using a smoothing function, GA(M)Ms can also capture non-linear short- and long-term trends while allowing to identify periods of strongly increasing or decreasing trends and breakpoints of (linear) trend direction (Fewster et al. 2000, Zuur 2012, Knappe 2016, Wood 2021).

We develop a user-friendly tool that integrates high observer turnover, long time gaps between successive surveys, spatial bias, as well as overdispersion and zero-inflation into an analysis of bird abundance trends from rolling surveys. It is exemplified with data from the Ecological Area Sampling (EAS), a monitoring programme of the German federal state North-Rhine Westphalia (NRW) with a six-

**Deleted:** Third, the distribution of breeding bird census data is often characterised by overdispersion and zero-inflation.

**Deleted:** the current

**Deleted:** standard

**Deleted:** -

**Deleted:** reaches its limits with substantial

**Deleted:** leading

**Deleted:** exceeding approx. 60 %

**Deleted:** still

**Deleted:** as well as changes in

**Deleted:** Here, we develop an analytical approach for monitoring designs that rely on rolling (or 'rotating') surveys with intervals of several years between repetitive surveys per site (Buckland and Johnston 2017). Rolling surveys can cover more study sites and thus a wider range of landscape types across years, but they also accept frequent observer changes and produce a high fraction of study sites with missing values each year. Given a lack of adequate modelling approaches for such monitoring programmes, we

**Deleted:** , to produce reliable and robust estimates

**Deleted:** breeding

**Deleted:** . The approach

165 year rolling sampling scheme. As a quality check, we compared the predicted population trends with West German trends derived from the German Common Bird Monitoring scheme (MhB) with yearly surveys per site. The statistical approach is provided as an R script (Rieger et al. 2025) and package (Rieger 2024) that can be adjusted to other datasets with a comparable structure.

Deleted: (Rieger et al. 2024)

## 170 2 Material and Methods

### 2.1 The Ecological area sampling (EAS) dataset

The Ecological Area Sampling (EAS) is a long-term biodiversity monitoring programme of the State Agency for Nature, Environment and Consumer Protection in North Rhine-Westphalia (LANUV) with 170 study sites that represent the average landscape of North-Rhine Westphalia (NRW) (LANUV 2016b). Sites are distributed across two biogeographic regions (atlantic lowlands, continental highlands) and six natural regions (Fig. 1) proportional to their spatial coverage. Another 21 metropolitan sites were added in 2011 to represent landscape characteristics of the Rhine-Ruhr metropolis region (Weiss and Schulze-Hagen 2014). The program targets an alternating six-year cycle for successive surveys of a given site, but could not yet strictly impose it given restructuring in the yearly balance of sites among natural and metropolitan regions (see section 2.3). The dataset for the survey period 2002-2020 typically covered 25 to 36 (max. 43 and 47) sites per year, two to four replicated surveys per site, and 614 surveys in total. Each site is visited at least nine times per sampling year (two to eight hours per date) between February and July with complete coverage of its 1 km<sup>2</sup> area (LANUV 2016a). The repetitive surveys are used to derive the territory count per species and km<sup>2</sup>, which represents the response variable abundance in all statistical analyses (LANUV 2016a). Survey effort (survey number and duration) constitute relevant model covariates but the respective information is not available for the current dataset (Further detail on EAS methodology, in appendix section 1).

Deleted: Our case study dataset originates from the

Deleted: ),

Deleted: sites are surveyed in

Deleted: resulting in a sample size of

Deleted: exceptionally up to

Deleted: or

Deleted: for the survey period 2002-2020

Deleted: These

Deleted: number of territories for each

Deleted: per

Deleted: For further details about

Deleted: , see

Deleted: .

### 2.2 Site characterization

190 Site-specific categories included biogeographic region (atlantic, continental), natural region (six regions as specified in Fig. 1), and localisation within a metropolitan area (no, yes). For analyses, we merged these into seven landscape types consisting of the six natural regions (sites outside the metropolitan area) and one metropolitan region (sites within the metropolitan area, ignoring natural regions given the overriding effect of urbanization in these lowland sites). Quantitative site characteristics included altitude above sea level (ATKIS 2013), ten parameters of climate and three of landscape compositions to account for variation in mean environmental attributes between the site subsets surveyed per year. Climate parameters included long-term spring and winter averages between 1981 and 2010 (CDC 2010)

Deleted: A, B, KB, KM, SB, ST, cf.

Deleted: in the

Deleted: covered the

Deleted: climate

Deleted: biases that arise from

Deleted: surveyed

of minimum, mean, and maximum temperatures, precipitation, and sunshine duration. Landscape variables were the coverages of forest, arable land, and settlements (ATKIS 2013). Given substantial collinearity between these 14 attributes, we integrated their principal components (PC) with eigenvalues exceeding 1 into the statistical models (three PCs in our case; for details see Appendix section 2).

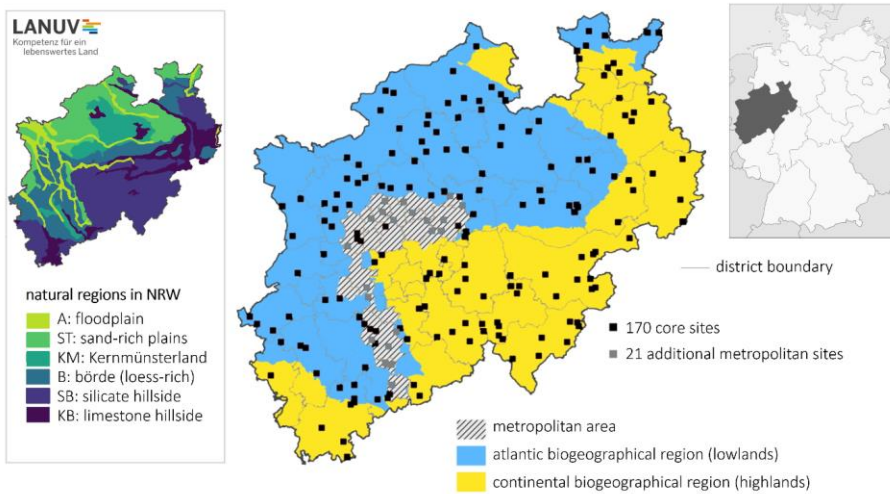


**Figure 1:** Sites and study area of EAS coloured by six natural regions (left) and two biogeographic regions including the Rhine-Ruhr metropolis (middle). Map adapted from LANUV (2016b).

### 2.3 Spatial bias

The initial sample of 170 EAS monitoring sites almost perfectly represented the proportional coverage of landscape types in NRW, but sampling bias arose from two sources. First, the monitoring programme added 21 metropolitan sites overrepresenting the metropolitan area to the other six landscape types in 2021. Second, the yearly subsampling of sites was highly unbalanced with respect to landscape types in the early phase of the EAS programme (Fig. 2), with improvements since 2007 and almost perfect balance since 2013.

To account for the uneven allocation in early programme years and for the overrepresentation of metropolitan areas since 2011, we analysed annual trends per landscape type.

**Deleted:** , each for spring and winter.

**Deleted:** coverage

**Deleted:** conducted a Principal Component Analysis and

**Deleted:** all

**Deleted:** –

**Deleted:** further

**Deleted:** source:

**Deleted:** additionally included

**Deleted:** without balanced sampling across

**Deleted:** required

**Deleted:** the combination of natural regions and metropolitan area (Fig. 2)

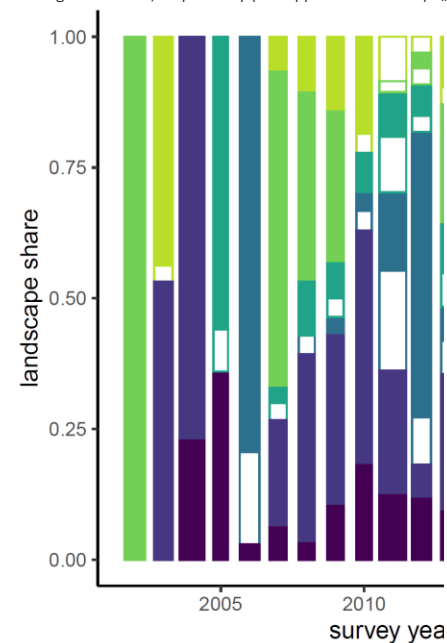
**Deleted:** ,

**Deleted:** (Fig. 2).

**Deleted:** weighted response measures accordingly. Weights per site and year were calculated as

$$\text{Deleted: weight} = \frac{TS_l}{AS_{lj}}$$

with  $TS_l$  the target share per landscape  $l$  (= proportional landscape cover in NRW) and  $AS_{lj}$  the actual share (= proportion of sites of the given landscape  $l$ ) among all surveyed sites in year  $j$  (Rieger 2024). A match between sample share and landscape coverage in NRW results in weight = 1, over- or underrepresented sample shares result in weights <1 or >1, respectively (see Appendix section 3).



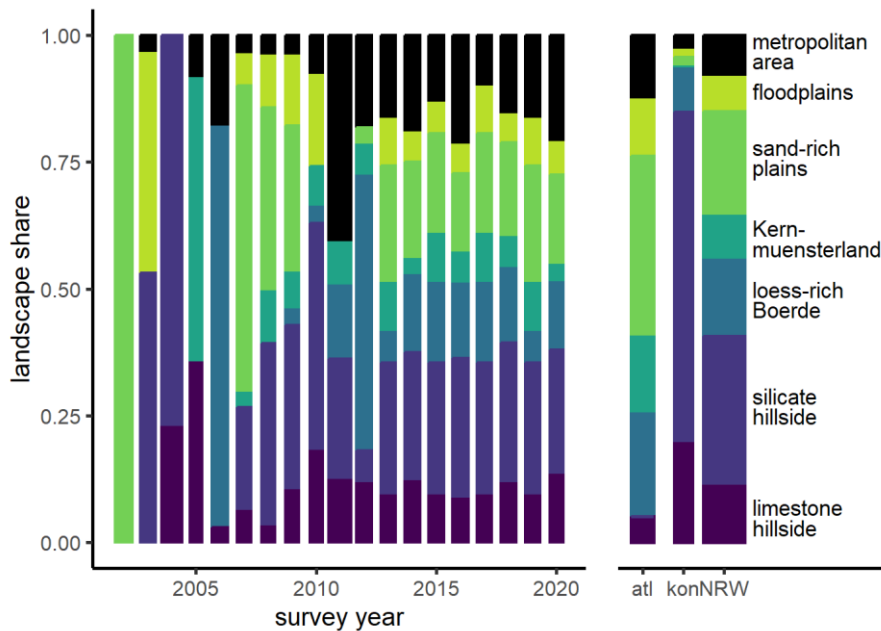


**Figure 2:** Landscape shares in annual EAS samples (main panel) and their spatial coverage *per biogeographical region and in NRW* (right panel). Bar widths are proportional to the number of surveyed sites per year.

## 2.4 Observer effects

The delineation of breeding territories is prone to under- and overestimation arising from variation in observer expertise *in species identification and detection*, territory delineation, and *general* field survey quality (Südbeck et al. 2005, Johnston et al. 2018), even in programmes such as *the* EAS that hire skilled ornithologists (König 2020). Observer effects add further noise to *trend estimates* when observers change *between successive surveys of a given* site. Excluding data from first year surveys, an established standard in monitoring data with yearly site coverage (e.g., German Common Bird Monitoring (Kamp et al. 2021)), is unfeasible for rolling surveys: In the EAS dataset, 434 out of 614 breeding bird surveys between 2002 and 2020 (71 %) were such first-year combinations of observer and site. *To characterise observer expertise and learning effects, we therefore categorized observers as (i) unfamiliar with the survey programme and site, (ii) familiar with survey programme but unfamiliar with the site, or (iii) familiar with both. Yet, we excluded this predictor from final models since it did not improve model fit, most likely because site familiarization introduced no detectable bias into the EAS trend estimates given the high observer turnover rates among successive surveys.*

Instead, we *identified* surveys with suspiciously high or low territory counts *summed across all species*. The procedure assumes that severe observer effects typically manifest in a general under- or

**Deleted:** ) for all combinations of natural regions and metropolitan area....

**Deleted:** White boxes at the lower end of each landscape refer to sample sites in metropolitan areas. \*metropolitan area of landscape not present in EAS due to low shares in NRW (SB = 0.4%, KB = 0.6%).

**Deleted:** monitoring data

**Deleted:** within

**Deleted:** delineated

overestimation of territory numbers (= abundance), so that total abundance (summed across species) for a given site and year stands out against average total abundance for that site. Based on this logic, we calculated

$$\text{Observer effect} = \frac{N_{js}}{\bar{N}_s}$$

with  $N_{js}$  the total abundance across species on site  $s$  in survey year  $j$ , and  $\bar{N}_s$  the mean total abundance across species on site  $s$  across all survey years (Rieger 2024). This observer effect is a ratio, so that a value of 1 indicates no deviation from the mean, and a value of 0.75 (1.25) a deviation of -25% (+25%) from the observed mean. We integrated the *observer effect* as a categorical predictor variable classified as 'negative' (or 'positive') when the abundance sum of a given survey was at least 25% smaller (or larger) than the mean per site, and as 'none' otherwise. As a sensitivity analysis, we also checked observer effect thresholds of 20% and 15%.

## 2.5 Distribution characteristics and the statistical analysis of EAS

We analysed species-specific abundance trends between 2002 and 2020 for all species with  $\leq 90\%$  zero-sightings among the 614 surveys (and thus at least 61 non-zero records) to allow plausible trend detection. The criterion was fulfilled in 61 (out of 148) species. For conciseness, this study focuses on a subset of 14 species that cover the observed range of abundance distributions and proportions of zero counts (Table 1).

Trends in Abundance, i.e. the territory count per site and year, were analysed using generalized additive mixed models (GAMMs) within a Bayesian framework as implemented in the package *brms* (v.2.21.0 (Bürkner 2017)) for R (v.4.3.3 (R Core Team 2024)). The *brms* package fits Bayesian models using *Stan* via the package *cmdstanr* (v.0.7.1 (Gabry and Češnovar 2020)) and allows to more flexibly integrate the required error families and model structures. We implemented four different error structures to account for zero-inflation or overdispersion, namely a Poisson error structure (Pois), negative binomial (nb), zero-inflated Poisson (zip), or zero-inflated negative binomial (zinb), all using a log link (Table 2, Appendix section 3). Since the underlying survey method generates .5 abundances for peripheral territories, we multiplied abundance by two (so it would be number of territories for 2 km<sup>2</sup>) and added an offset of two to all models.

The main model was constructed as follows, and we explain each model component below:

$$2 * \text{Abundance} \sim s(\text{Year}, \text{by} = \text{Landscape}) + \text{Landscape} + \text{Observer} \\ + \text{poly}(\text{PC1}, 2) + \text{poly}(\text{PC2}, 2) + \text{poly}(\text{PC3}, 2)$$

**Deleted:** ) across species,

**Deleted:**  $AB_{js}$

**Deleted:** sum

**Deleted:**  $\bar{AB}_s$

**Deleted:** sum

**Deleted:** The

**Deleted:** As an alternative way to characterise observer expertise and learning effects, we categorized observers as (i) unfamiliar with the survey programme and site, (ii) familiar with survey programme but unfamiliar with the site, or (iii) familiar with both. Yet, we excluded this predictor in final models since it did not improve model fit, most likely because observer turnover rates were high and thus site familiarization effects unlikely to introduce relevant bias into the EAS trend estimates.¶

**Deleted:** population

**Deleted:** the entire federal state for

**Deleted:** a proportion of

**Deleted:** below 90%

**Deleted:** both biogeographic regions (61

**Deleted:** ), and for just the Atlantic or continental region for species that met this criterion only in one of the two biogeographic regions (24 out of 148). For clarity and

**Deleted:** selected to

**Deleted:** full

**Deleted:** Breeding bird abundance trends

**Deleted:** of the statistical software

**Deleted:** than current frequentist GAMM packages such as *mgcv* (Wood 2021) or *gamm4* (Wood and Scheipl 2020)). Initial models implemented a Poisson error structure with a log-link (Fig. 3, Table 4). Where species-specific model assessment implied excessive zero frequencies or overdispersion of the response variable abundance, we chose zero-inflated negative binomial (zinb), zero-inflated Poisson (zip) or negative binomial (nb) models as needed (Fig. 3, Table 2, Appendix section 5). Since the underlying survey method can lead to 0.5 abundances due to peripheral territories, decimal raw abundances were rounded to the next integer (see Appendix section 1). Given non-representative sampling across landscapes, we weighted the abundance by the factor defined in section 2.3

**Deleted:** All abundance models had



+ offset(log(2)) + (1|siteID). (1)

365 Survey Year as the main continuous predictor was modelled with a smoothing function (thin plate regression splines with an automatic selection of the degree of smoothing) to account for non-linear changes in abundance over time, while allowing adjacent years to be related to each other (Fewster et al. 2000, Zuur 2012, Knappe 2016, Wood 2021). Thus, smoothers buffer against the property of rolling surveys that sampled site subsets differ between successive years, so that year-to-year changes in abundance cannot differentiate among-site variation from true short-term change in population size (Zuur 2012). Smoothers were modelled separately per Landscape type to account for spatial bias due to the unbalanced sampling design (Fig. 2).

375 We added Landscape type as a categorical main effect, (Wood 2021), to contrast population densities and trends between the seven landscapes. Landscape types showed near-complete separation between biogeographical regions, where the continental region encompasses the natural regions 'silicate hillside' and 'limestone hillside' and the Atlantic region the remaining five natural regions including the 'metropolitan area'. We therefore refrained from adding biogeographic region as a separate predictor, but extract population trends per biogeographic region by combining the respective landscape trends (see section 'Population trends').

380 Observer effects as outlined in section 2.4 were added as a categorical covariate. For numeric covariates, we included linear and quadratic terms of site-specific environmental attributes captured in the first three principal components PC1 to PC3 as outlined in section 2.2 and Appendix section 2. Finally, we added site-ID as a random intercept to reflect repeated measures per site and to model variation in mean abundance between the different site subsets per year.

385 The zero-inflation model component, where needed (Table 1), represents a binomial (Bernoulli) model with a logit link to estimate the additional occurrence of structural zeros. We kept this component as simple as possible, (formulation 2.1) and estimated separate zero-inflation parameters per Landscape type, environmental PC, or study site-ID (formulations 2.2–2.4) only where needed to improve model convergence and better reflect the observed distribution of zero counts (Fig. 3, Table 2):

390 zi-formula ~ 1 (2.1)

zi-formula ~ Landscape (2.2)

zi-formula ~ PC1 + PC2 + PC3 (2.3)

zi-formula ~ (1|siteID) (2.4)

**Deleted:** year

**Deleted:** (i)

**Deleted:** ,

**Deleted:** (ii) still

**Deleted:** To estimate regional population densities and trends as well as their differences, we

**Deleted:** biogeographic region

**Deleted:** to obtain separate smoothers for the Atlantic and continental region

**Deleted:** . Due

**Deleted:** a non-overlap of natural regions

**Deleted:** (the Atlantic region mainly consisted of floodplains, sand-rich plains, loess-rich Boerde, and chalk-rich Kernmuensterland, whereas

**Deleted:** mainly consisted of

**Deleted:** hillside), we refrained from adding

**Deleted:** as a further predictor. Models

**Deleted:** cannot provide

**Deleted:** trend and density estimates

**Deleted:** natural region but integrate corrections for non-representative sampling of natural regions through the weighting factors introduced above.

**Deleted:** Numeric

**Deleted:** (sections 2

**Deleted:** ) to account for bias that arises from variation in mean environmental attributes between the surveyed site subsets per year....

**Deleted:**

**Deleted:** , adding

**Deleted:** PCs, biogeographic region, and the random intercept...

**Deleted:**

**Deleted:** as

**Deleted:** ).

**Deleted:** There was no need to integrate temporal autoregressive structures into models since visual inspection of...



We did not integrate temporal autoregressive structures (van Strien et al. 2004, Korner-Nievergelt et al. 2015) because variograms plotted with the *variog* function of the package *geoR* (v.1.9-3 (Ribeiro Jr and Diggle 2020)) revealed no issues with temporal autocorrelation. This may result from the six-year gaps between repeated measures (usually accompanied by a change in observer), which may add more variation to model residuals than expected from the remaining temporal pattern, rendering temporal autocorrelation negligible.

**Table 1:** Overview of model types (main model family, coefficients in the optional zi-binomial model) and number of case study species per model type. Species names are given for the 14 exemplary species shown in this paper. Details for all species are in Appendix section 7. Models are ordered according to their parsimony (top = most parsimonious).

model family	binomial model coefficients	# species (%)	exemplary species
pois		3 (4.9%)	European Green Woodpecker ( <i>Picus viridis</i> ), Eurasian Nuthatch ( <i>Sitta europaea</i> )
nb		13 (21.3%)	Eurasian Blue Tit ( <i>Cyanistes caeruleus</i> ), Common Chiffchaff ( <i>Phylloscopus collybita</i> )
zip	~ 1	7 (11.5%)	Black Redstart ( <i>Phoenicurus ochruros</i> ), Willow-Tit ( <i>Poecile montanus</i> )
zinb	~ 1	13 (21.3%)	Great Tit ( <i>Parus major</i> )
zip	~ PCs	3 (4.9%)	Grey Wagtail ( <i>Motacilla cinerea</i> )
zinb	~ PCs	6 (9.8%)	Eurasian Jay ( <i>Garrulus glandarius</i> ), Common Chaffinch ( <i>Fringilla coelebs</i> )
zip	~ 1	1 (1.6%)	Common Kestrel ( <i>Falco tinnunculus</i> )
zinb	~ 1	3 (4.9%)	Barn Swallow ( <i>Hirundo rustica</i> )
zip	~ (1 ID)	5 (8.2%)	Common Buzzard ( <i>Buteo buteo</i> )
zinb	~ (1 ID)	7 (11.5%)	Eurasian Magpie ( <i>Pica pica</i> )

pois = Poisson, nb = negative binomial, zip = zero-inflated Poisson, zinb = zero-inflated negative binomial, PCs = Principal Components PC1 + PC2 + PC3, 1 = Landscape type, (1|ID) = random intercept of site ID.

To fit Bayesian models, we used weakly informative prior distributions for coefficients (normal with mean = 0, SD = 2.5 for categorical coefficients, mean = 0, SD = 10 for numeric coefficients) and a maximum tree depth of 10. Each model ran four Markov chain Monte Carlo chains with 1,000 warm-up and 2,000 post-warm-up samples per chain. We used the 8,000 post-warm-up samples for posterior predictive checks of the models' ability to simulate the observed abundance distribution. Criteria included distributional characteristics (mean and standard deviation) as well as the model's ability to reflect extreme values (maximum value) and potential zero inflation (proportion of zero counts, propZ) in the data. In all these cases, we calculated the proportion of simulations exceeding the observed raw data value (Bayesian p-value, Korner-Nievergelt et al. 2015). Bayesian p close to 0.5 imply a good match because the observed values are roughly central within the distribution of simulated data, while values approaching 0 or 1 flag models that clearly under- or overestimated the observed value.

**Deleted:** , probably because... This may result from the six-year gaps between repeated measures (usually accompanied by a change in observer) added..., which may add more variation to model residuals than expected from the remaining temporal pattern, rendering any remaining

**Deleted:** For further details of...etails for all species, see...are in Appendix section 9.

**Deleted:** Common Kestrel (*Falco tinnunculus*), 1

**Deleted:** 19 (22).

**Deleted:** Jay (*Garrulus glandarius*)

**Deleted:** 4 (4.7)

**Deleted:** Blackbird (*Turdus merula*)

**Moved down [1]:** Common Chaffinch (*Fringilla coelebs*)

**Deleted:** zip 1

**Deleted:** R

**Deleted:** 1 (1.2)

**Deleted:** 1

~ PCs

**Deleted:** (...|ID)

**Deleted:** 5 (5.9)

**Deleted:** Spotted Woodpecker (*Dendrocopos*)

**Deleted:** 1

~ R + (1|ID)

**Deleted:** + (1|ID)

**Deleted:** 8 (... (4.9.4)

**Deleted:** White...rey Wagtail (*Motacilla alba*)

**Moved (insertion) [1]**

**Deleted:** PCs + R + (1|ID)

**Deleted:** 2

**Split Cells**

**Deleted:** 1

**Deleted:** 3.5

**Deleted:** Eurasian Blackcap (*Sylvia atricapilla*)

**Deleted:** R

**Deleted:** 3 (3).

**Deleted:** Chiffchaff (*Phylloscopus collybita*)

**Deleted:** PCs

**Deleted:** 8.2

**Deleted:** 1

~ (1|ID)

**Deleted:** R = biogeographic region, OE = observer effect... = Landscape type, (1|ID) = random effect

**Deleted:** eight...our Markov chain Monte Carlo chains with 1500...,000 warm-up and 4000...,000 post-warm-up samples per chain. The 32000...e used the 8,000 post-warm-up samples were used to assess model fit via...or posterior

We further checked several conversion indicators of the coefficient estimates:  $R_{\text{hat}}$ -values  $\leq 1.1$  (observed max = 1.01) (Brooks and Gelman 1998), effective posterior samples  $\geq 10\%$  of total samples (observed min = 9.4%) and Monte Carlo standard errors  $\leq 10\%$  of the standard deviation (observed max = 4.3%) (Korner-Nievergelt et al. 2015). To select the model with the best predictive performance per species, we did a k-fold-cross-validation using 16 folds resulting in a theoretical expected log pointwise predictive density (ELPD) per model, as well as ELPD differences (model with best ELPD compared to others) and the respective standard error of the difference (se ELPD difference) (Bürkner 2017). When several models resulted in near-identical performance (ELPD difference  $\pm 1.96 \cdot \text{se ELPD difference}$  included 0), we continued with the most parsimonious model, i.e., the model with the lowest number of covariates or model components (see Table 1), that fulfilled our conversion indicators.

From the post-warm-up samples we also derived mean covariate coefficient estimates with their 95% credible intervals (Crl) and the posterior probability that the estimate exceeds 0,  $P(\beta > 0)$ . Posterior probabilities approaching 0 or 1 indicate increasingly strong evidence for a directional coefficient.

### Population trend

Model predictions  $\pm 95\%$  Crl were derived via `brms.fitted` (Bürkner 2017) to display trends graphically. When estimating trends over years and differences between landscape types, values of the remaining model covariates were set to their landscape-specific sample mean (continuous covariates), to the level 'none' (for 'observer effect') (Korner-Nievergelt et al. 2015), and group-level effects ('site ID') were generalized beyond the specific grouping level by using the argument `re_formula = NA`. We derived trends across biogeographic regions by combining these landscape-specific trends according to the landscape's share of the biogeographic region (Atlantic (continental): A = 11.7% (2.1%), B = 20.9% (9.2%), KB = 5.1% (20.1%), KM = 15.1% (0.4%), SB = 0.0% (64.7%), ST = 35.1% (1.2%), metro = 12.1% (2.3%). Overall trends were derived alike by combining the region-specific trends according to their share of NRW (55.5% Atlantic region and 44.5% continental region). Based on pairwise differences of simulated abundances, we estimated trends as changes in abundance between the start and end date of any desired time period as

$$\text{Pairwise difference} = N_{ij} - N_{i(j-\Delta t)}$$

with  $N$  the predicted abundance for the  $i$ th posterior draw at times  $j$  and  $j - \Delta t$ , where  $\Delta t$  is the desired time period. If the 95% Crl of these simulated differences excluded 0, the trend estimate was considered robust. We specifically produced pairwise differences to estimate annual changes ( $\Delta t = 1$ ) and a 12-year trend between 2008 and 2019 ( $\Delta t = 12$ ,  $j = 2019$ ).

**Deleted:** Selection value =  $\sum (0.5 - B_{\text{run}})^2$  with  $B$  the Bayesian p-value for the four different functions

**Deleted:** *propZ*, *mean*, *max*, and *SD* (Rieger 2024). Values close to 0 indicate good model performance with only minor deviations from the ideal Bayesian p-values, values close to 1 indicate poor model performance (see also section 3.1 and Appendix section 5).  
The

**Deleted:** were

**Deleted:** used to derive

**Deleted:** for all covariates

**Deleted:** as well as

**Deleted:** (postP) of

**Deleted:** to exceed 0.

**Deleted:** rather robust

**Deleted:** estimates

**Deleted:** used

**Deleted:** across survey

**Deleted:** biogeographic regions

**Deleted:** ) and

**Deleted:** .

**Deleted:** overall

**Deleted:** region

**Deleted:** region's

**Deleted:**  $ab_{ij}$

**Deleted:**  $ab$

**Deleted:**  $ab$

**Deleted:** simulation

**Deleted:** fine-scale changes in trend slopes ( $\Delta t = 0.001$ ),

**Deleted:** ),

**Deleted:** to

## Population index

For comparison with other monitoring programmes, we integrated the option to transform predicted mean abundances per km<sup>2</sup> into an index relative to a user-selected baseline year (here: 2006). Even though the first few years of the monitoring programme suffer from non-representative sampling (see section 2.3), weights and smoothing-function enabled accurate estimates in these years without distorting successive estimates (Buckland and Johnston 2017). Abundance indices were calculated as

$$\text{Abundance index} = \frac{N_{ij}}{\bar{N}_j}$$

with  $N_{ij}$  the predicted abundance of the  $i$ th posterior draw in year  $j$ , and  $\bar{N}_j$  the mean predicted abundance of all simulations in the baseline year  $J$  (here  $J = 2006$ ). Based on 10,000 simulations, we calculated the mean index and its 95% CrI for each time step  $j$ . Note that this computation calculates an uncertainty also for the baseline year  $J$ . Users who prefer a fixed baseline year index without uncertainty need to replace the mean abundance denominator,  $\bar{N}_j$  in the formula by  $N_{iJ}$ , i.e. the  $i$ th simulation in the baseline year.

## Data exclusion

Based on an internal validation process of the LANUV, some abundance data were classified as implausible and therefore excluded from the analysis. This process was species-dependent, leading to sample sizes of 608 to 614 per species (full dataset: 614, Appendix section 7).

## 2.6 Consistency check

We checked our EAS trends for NRW for consistency with population trends in all West Germany according to the German Common Bird Monitoring scheme (MhB), coordinated by the German association for field ornithologists (DDA). MhB study sites are ideally surveyed each year by the same observer (four surveys per site between 10 March and 20 June; full programme details in Kamp et al. (2021)).

The consistency analysis included 59 widely distributed species spanning a broad range of habitat associations and breeding strategies for which we had trend estimates available from the MhB and from the EAS. It is obviously difficult to compare trend estimates between programmes that rest on different methodologies and survey efforts (nine vs. four surveys per year), have different spatial coverage (NRW

**Deleted:** trend comparisons

**Deleted:** poor representativity

**Deleted:** following

**Deleted:**  $ab_{ij}$

**Deleted:** simulation

**Deleted:**  $\bar{ab}_j$

**Deleted:** 32000

**Deleted:** 9). Weights were derived from these revised datasets.

**Deleted:** as well as for both biogeographic regions in

**Deleted:** We expected that even such structured monitoring programmes should generate largely consistent trend estimates when sufficiently robust, except for well justified cases. We calculated two parameters for each species: first, a Pearson 'correlation' coefficient between the annual TRIM-based MhB indices and the annual EAS-indices extracted from model smoothers between 2005 and 2020; second, an index of 'coincidence' as the fraction of annual MhB index values that fell within the 95% CrI of EAS-derived indices. ¶

**Deleted:** with

**Deleted:** with

**Deleted:** target scales

vs. West Germany) with just a partial match in study sites, and employ fundamentally different analytical approaches (GAM smoothers in EAS vs. yearly point estimates in MhB). Nevertheless, largely consistent estimates from EAS and MhB would reassure that the analytical approach developed for rolling sampling strategies produces reliable trends that are robust to the underlying survey design. With these limitations in mind, we expected that yearly samples in the MhB versus 6-yearly samples in the EAS should generate largely consistent long-term trend estimates, except for cases where a species' biology would objectively favour one survey and analysis routine over the other (see Discussion).

To assess trend consistency we calculated two parameters for each species: (i) a Pearson 'correlation' coefficient between the annual TRIM-based MhB indices and the annual EAS-indices extracted from model smoothers between 2005 and 2020, and (ii) the Median Symmetric Accuracy (Morley et al. 2018), which estimates the median percentage error between both annual indices  $I_j$ :

$$\text{Median Symmetric Accuracy} = 100 * \exp \left( \text{median} \left( \text{abs} \left( \log \left( \frac{I_{MhBj}}{I_{EASj}} \right) \right) \right) \right) - 1$$

Note that the baseline year 2006 (both indices = 1) was excluded for both methods.

### 3 Results

Breeding bird trends were analysed for 61 out of 148 bird species (full detail in Appendix section 6, 7), but we focus the description of model assessment results on 14 exemplary species (tab. 1). Exemplified data for five species, script, and code are available from Github ([https://github.com/m-rieger/EAS\\_bird](https://github.com/m-rieger/EAS_bird)) (Rieger et al. 2025) as well as a package with helper functions (<https://github.com/m-rieger/EAS>) (Rieger 2024).

#### 3.1 Distribution characteristics: Species-specific optimisation

Model selection via k-fold cross validation resulted in different best-performing model families and a species-specific selection of coefficients added to the binomial part of zero-inflated models (Table 1, species-specific overview in Appendix section 7). We illustrate below the selection of model structure on four species that strongly vary in overall mean abundance, abundance dispersion, and the proportion of sites with zero counts: European Green Woodpecker, Eurasian Blue Tit, Black Redstart, and Eurasian Jay. The four measures that inform abundance distribution (propZ, mean, SD, max) can – but do not necessarily need to – vary with each other, so that an over- or underestimation of zero counts often goes along with an under- or overestimation of the population mean, and an over- or underestimation of SD with an over- or underestimation of maximum abundance.

Deleted: coupled

Deleted: regional coverage, and with such

Deleted: trend

Deleted: the far more variable

Deleted: 85

Deleted: 8, 9

Deleted: (Rieger et al. 2024)

Deleted: optimisation

Deleted: 9). When several models resulted in comparably good performance, we continued with the most parsimonious model, i.e., the model with the lower number of covariates or model components.

Deleted: with striking differences

Deleted: Common Kestrel

Deleted: Blackbird, White Wagtail

Deleted: Common Chiffchaff.

Deleted: model optimisation

**Table 2:** Examples for model assessment and procedure to select species-specific models from six alternative model structures (for further species and models see Appendix section 3). Models differ in family and the presence of a zero-inflated model component (zinb and zip), the latter also in binomial model coefficients. Model assessment quantifies whether simulated data from the model is consistent with the observed response variable (abundance) with respect to its proportion of zeros (propZ), mean and maximum value, and standard deviation (SD). Bayesian p-values close to 0.5 indicate that the observed values are central within the posterior distribution of simulated raw datasets (8000 in total), indicating good model fit. Values close to 0 and 1 indicate substantial under- or overestimation and thus poor model fit. Final model selection is based on ELPD differences by selecting the most parsimonious model (bold, top to bottom) out of all models with an ELPD difference  $\pm 1.96 \cdot \text{SE}$  of ELPD difference including 0 (bold values). Abbreviations see Table. 1.

species	model family	binomial model coefficient s	Bayesian p-value				ELPD	
			propZ	mean	SD	max	diff.	se diff.
European Green Woodpecker	pois		0.01	0.49	0.79	0.65	-11.86	7.89
	nb						-	
	zip	~ 1	0.12	0.44	0.87	0.72	-6.65	6.77
	zinb	~ 1	0.13	0.46	0.91	0.80	-8.06	6.73
Picus viridis	zip	~ PCs	0.16	0.46	0.88	0.71	-3.66	6.92
	zinb	~ PCs	0.16	0.48	0.90	0.76	-18.57	7.91
	pois						-	
	nb		0	0.50	0.01	0.02	510.17	69.13
Eurasian Blue Tit	zip	~ 1					-	
	zinb	~ 1	0.10	0.34	0.01	0.02	498.39	66.54
	zip	~ PCs	0.07	0.58	0.69	0.37	-19.9	8.09
	zinb	~ PCs	0.11	0.39	0.01	0.02	509.75	71.86
Black Redstart	pois		0	0.51	0.56	0.47	-23.37	10.14
	nb						-	
	zip	~ 1	0	0.59	0.82	0.59	3654.6	780.81
	zinb	~ 1	0	0.42	0.76	0.56	-4.01	7.52
Eurasian Jay	zip	~ PCs	0	0.42	0.54	0.48	-12.87	9.19
	zinb	~ PCs	0	0.51	0.79	0.51	0	0
	pois		0	0.50	0.76	0.77	-37.68	11.47
	nb						-	

- Deleted: Common Kestrel (Table 2, Fig. 3a) represents
- Deleted: 5... Models differ in family and the presence of
- Deleted Cells
- Deleted: selection value
- Split Cells
- Deleted: Species
- Deleted: propZ
- Deleted: mean
- Deleted: SD
- Deleted: max
- Split Cells
- Deleted: 71
- Deleted: 58
- Deleted: 91
- Deleted: 0.98
- Deleted: 0.46
- Deleted: 0.99
- Deleted: Common Kestrel
- Deleted: 72
- Deleted: 58
- Deleted: 92
- Deleted: 0.46
- Moved (insertion) [2]
- Deleted: R
- Deleted: 72
- Deleted: 58
- Deleted: 91
- Deleted: 0.99
- Deleted: 0.46
- Deleted: R
- Deleted: 73
- Deleted: 57
- Deleted: 92
- Deleted: 0.99
- Deleted: 0.47
- Deleted: + (1|ID)
- Deleted: 73
- Deleted: 64
- Deleted: 96
- Deleted: 0.99
- Deleted: 0.53
- Deleted: + (1|ID)
- Deleted: 75
- Deleted: 64
- Deleted: 96
- Deleted: 0.99
- Deleted: 0.53
- Deleted: 0.13
- Deleted: 52

1160

<u>Garullus</u>	nb								
<u>glandarius</u>		0	0.69	0.89	0.70		117.44	22.38	Deleted: 0.52
	zip	~ 1	0	0.31	0.78	0.76	-27.5	8.37	Deleted: 01
	zinb	~ 1	0	0.34	0.83	0.81	-28.52	8.11	Deleted: 66
	zip	~ PCs	0.19	0.36	0.77	0.67	-23.57	10.83	Deleted: 39
	zinb	~ PCs	0.19	0.39	0.81	0.72	-15.08	10.25	Deleted: 0.28
									Deleted: R
									Deleted: 27
									Deleted: 56
									Deleted: 09
									Deleted: 0.26
									Deleted: 0.28
									Deleted: R
									Deleted: 29
									Deleted: 60
									Deleted: 41
									Deleted: 0.50
									Deleted: 0.06
									Deleted: + (1 ID)
									Deleted: 26
									Deleted: 57
									Deleted: 09
									Deleted: 0.26
									Deleted: 0.29
									Moved up [3]: 0.07
									Deleted: + (1 ID)
									Deleted: 27
									Deleted: 60
									Deleted: 41
									Deleted: 0.51

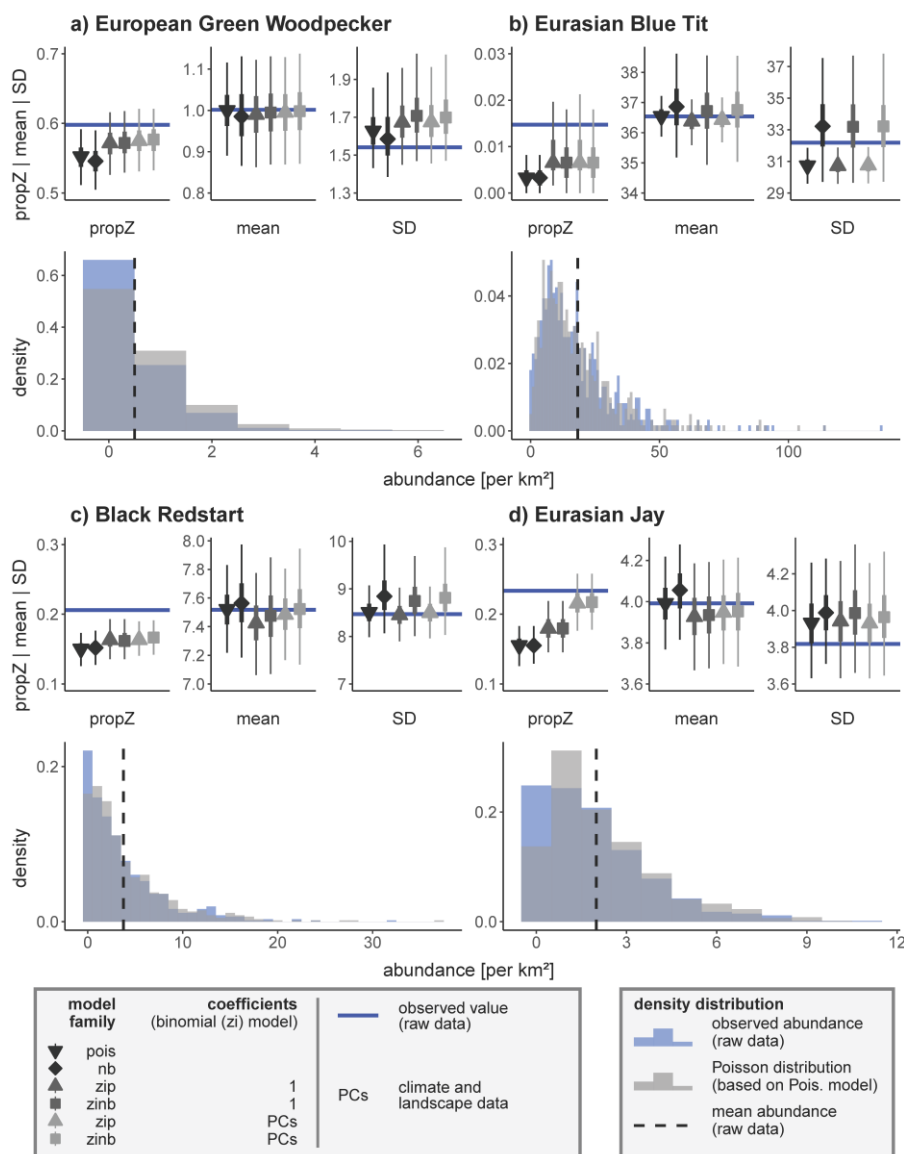


**Figure 3:** Reasoning for selecting appropriate model structures for four species. **Upper panels:** Model performance with respect to the proportion of zero counts (propZ), mean, and standard deviation (SD) of the response variable 'abundance'. Symbols with error bars display the median  $\pm$  50% CrI (thick bars) and 95% CrI (thin bars) for 8000 posterior raw datasets simulated from the selected models as given in the legend. Optimal models have a close match between observed and model-predicted data. **Lower panels:** Density distributions of observed abundances (blue, dashed line = mean) and Poisson distributions (grey) based on simulated responses derived from the respective Poisson model. Y-axes differ in scale.

Deleted: ¶

Deleted: 32000

Deleted: simulated

Deleted: observed

Deleted: mean abundance (dashed line). In many cases, the observed distribution is clearly wider than predicted by

Deleted: , indicating overdispersion.

Deleted:



1210 European Green Woodpecker (Table 2, Fig. 3a) represents species with typically low territory numbers and many zero counts. While all models underestimated the number of zero counts, a Poisson model sufficiently captured other distribution parameters, resulting in a good predictive performance.

1215 Eurasian Blue Tit (Table 2, Fig. 3b) is an abundant and widespread species that occurs in nearly all study sites. Here, abundance varied clearly more within sites and/or between year than reflected by a Poisson distribution. This issue of an underestimated SD was solved by using a negative binomial model family, even though leading to a slight overestimated SD.

1220 Black Redstart (Table 2, Fig. 3c) is widespread at typically medium densities, resulting in a larger fraction of unoccupied sites than expected under a Poisson distribution. All models failed to capture this zero-bias, but models with a zero-inflation component were closer to the observed value. Since zero-inflated models mostly resulted in comparable ELPDs, we used the most parsimonious model (zero-inflated Poisson with no additional binomial coefficient) for further analyses.

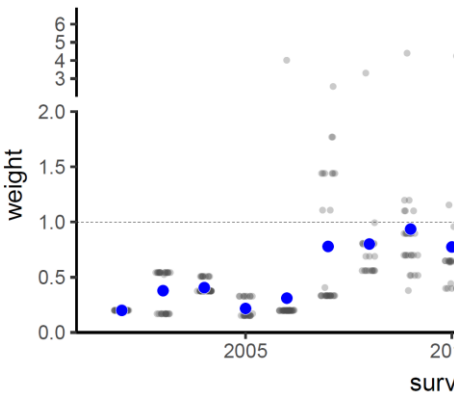
1225 Eurasian Jay (Table 2, Fig. 3d) is a widespread species with low territory numbers. Using zero-inflated models with environmental PCs as binomial model coefficient sufficiently captured the observed number of zero counts, and the zero-inflated negative binomial model resulted in the best predictive performance.

1225 3.2 Spatial bias

1230 For many species, (long-term) trends varied between landscapes, confirming the need to account for spatial bias. Especially long-term trends in metropolitan areas differed considerably from trends in other landscapes, usually showing steeper decreases (except for a steeper increase in Black Redstart, Fig. 4). Ignoring the overrepresentation of metropolitan sites (or any other unbalance in landscape samples) in the EAS dataset would therefore result in biased (long-term) trends for biogeographic regions and overall. In case of Eurasian Magpie and Eurasian Nuthatch, trends would be more negative and for Black Redstart more positive.

Moved down [4]: 3.2 Spatial bias¶

**Deleted:** Due to added weights, especially the early years in the EAS-period had less influence on the model than more recent years with a more balanced sampling distribution (Fig. 4, Fig. 2). Therefore, only recent years achieved a sufficient coverage (= mean weight) of almost 1, whereas the first five years did not even approach a coverage of 50% (Fig. 4). Additionally, there were single high weights between 2006 and 2012 (Fig. 4).¶



Moved (insertion) [4]

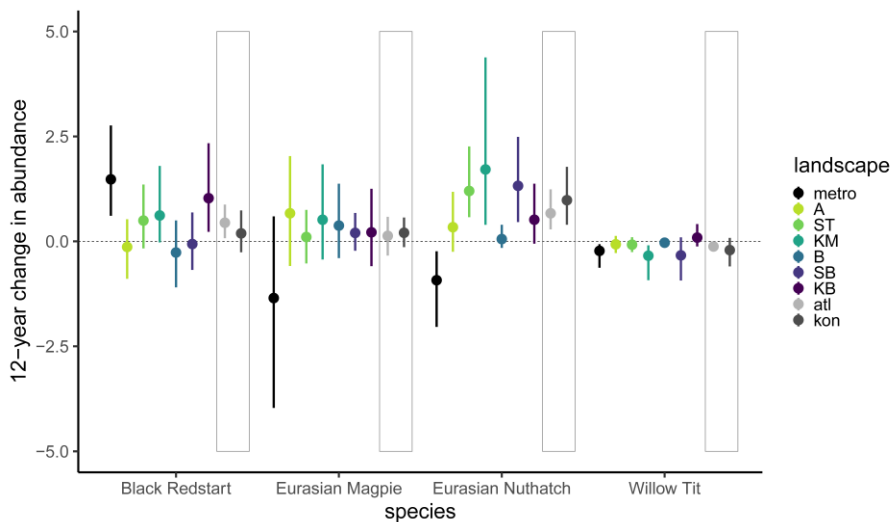


**Figure 4:** Long-term trends (2008-2019) per landscape and biogeographic region (atl, kon, grey box) for four example species. The y-axis displays the absolute change in abundance across 12 years (and not per year).

### 3.3 Observer effects

We found a strikingly inhomogeneous distribution of observer effects across years, bearing substantial potential for biased population trend estimates when unaccounted for. High total abundances occurred disproportionately often since 2015, and strikingly low abundances before 2006 (Fig. 5, left), irrespective of the chosen threshold value (Appendix section 4). Models ignoring observer effects generally produced more positive 12-year trend estimates, i.e., resulted in steeper increases or less steep declines than models with the covariate *observer effect* (Fig. 5, right). For Chaffinch, correcting for observer effects even reversed the increase in abundance in the non-corrected model to a decrease in the corrected model (Fig. 5, right). OE-corrected trend estimates were generally more consistent with West German trend estimates from the MhB programme (Appendix section 4) where consecutive surveys at a given site are always from the same observer.

**Deleted:** Weights per year and site (grey dots) as well as mean weight per year (blue dots). Sites within a

**Deleted:** share identical weights within years, resulting in bandings of dots. Note ...

**Deleted:** break. ¶

**Deleted:**  $\pm$  95% CrI for models with (blue) and without weights (grey) added to the response variable abundance, including raw data (grey dots) for Chiffchaff. Slopes substantially differing from 0 (see section 2.5) are highlighted

**Deleted:** 6

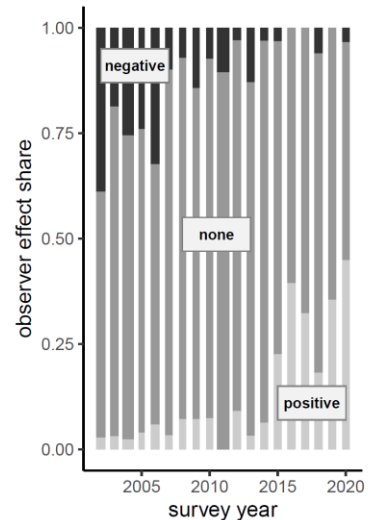
**Deleted:** 6

**Deleted:** 6

**Deleted:** 6

**Deleted:** form

**Deleted:** 6).



**Deleted:**

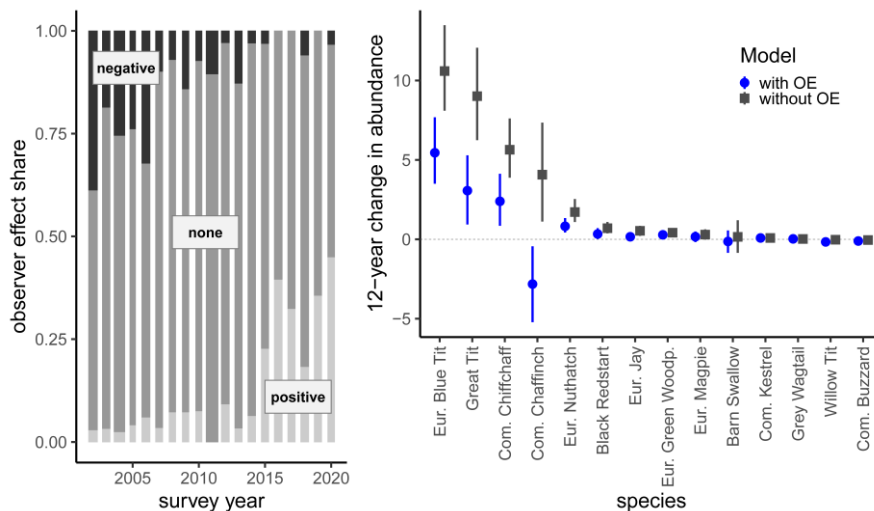


**Figure 5:** Left: Proportion of surveyed EAS sites per observer effect level per year. Bar widths are proportional to the number of surveyed sites per year. Right: 12-year change in abundance (2008-2019) estimated from models with and without the covariate observer effects (OE) for 14 species (example trend curves in Appendix section 4). The y-axis displays the absolute change in abundance across 12 years (and not per year).

### 3.4 Consistency check

Correlation coefficients between annual EAS indices and West German MhB indices revealed solid matches – i.e., with correlation coefficients and their 95% CI  $> 0$  – for 34 out of 59 species (e.g., Nuthatch and Chiffchaff in Fig. 6a, b). Only five species (e.g., Eurasian Jay in Fig. 6d) tended to have negatively correlated yearly indices, but correlation coefficients and 95% CI always included 0. Likewise, median symmetric accuracy (MSA) values between index estimates were reasonably low, with 43 (26) out of 59 species deviating  $\leq 20\%$  (10%). High correlation not necessarily goes along with low MSA values, because the latter are sensitive to the index baseline year as illustrated by the Chiffchaff data (Fig. 6b). Here, EAS- and MhB-analyses generate a nicely consistent trend pattern, but MSA was high because the exceptionally low MhB index in the baseline year 2006 distorts almost all other annual MhB-index values to exceed the EAS values, resulting in different magnitudes of change. In contrast, Great Tit and Eurasian Jay exemplify how poor correlation between annual index values can go along with low MSA values (Fig. 6c, d), here because a rather stable vs. more fluctuating trend (Great Tit) that is identified by a weak correlation shows only minor deviations in trends (low MSA) or largely overlapping but slightly diverging trends (Eurasian Jay, especially due to year 2005) fail to correlate. Correlation coefficients, MSA values, and trend displays for all 59 species are in Appendix section 5.

Deleted: 6

Deleted: (circles, blue)

Deleted: (squares, grey)

Deleted: 6

Deleted: ,

Deleted: ,

Deleted: 37

Deleted: Blackbird

Deleted: 7a

Deleted: one

Deleted: Common Swift, Appendix section 7) showed

Deleted: with

Deleted: coefficient

Deleted: <

Deleted: coincidence

Deleted: was

Deleted: high

Deleted: 55 (47)

Deleted: having  $\geq 75\%$  (90%) of the annual mean MhB indices within the 95% CrI of the respective annual EAS index.

Deleted: a high coincidence index

Deleted: is

Deleted: 7b

Deleted: our coincidence index fails

Deleted: credible intervals.

Deleted: high index coincidence

Deleted: 7c

Deleted: is hidden within the broad credible intervals of the EAS trend estimate...

Deleted: coincidence

Deleted: 7

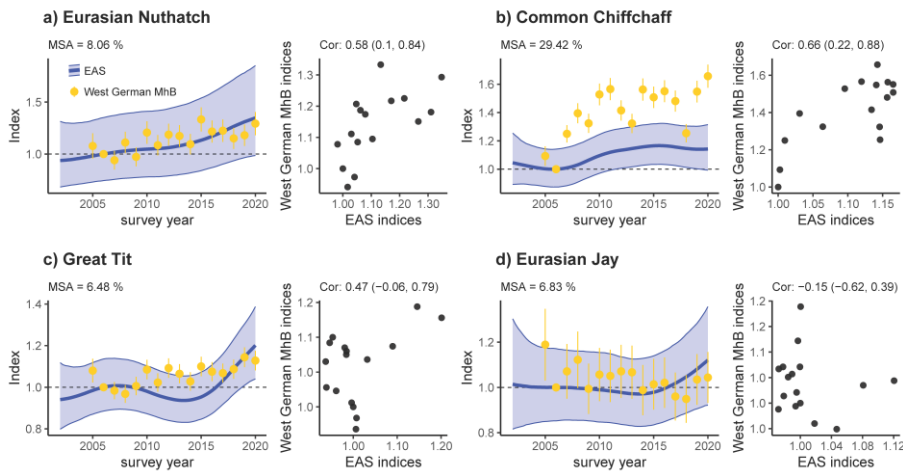


**Figure 6:** Trend comparison of EAS monitoring programme and West German MhB for four species. Left (per panel): Median Symmetric Accuracy (MSA) based on annual comparisons of indices. Right (per panel): correlation and correlation coefficients ( $\pm$  95% CI) of annual indices from 2005 to 2020. Both approaches exclude the baseline year 2006.

## 4 Discussion

Count data are the raw unit for many population trend analyses, but their distribution poses several challenges during statistical analyses to account for overdispersion (42 out of 61 species in our current dataset) and/or zero inflation (45 out of 61 species). Moreover, many biodiversity monitoring programmes rest on ‘rolling’ sampling designs where each study site is visited only every so many years and observer identity frequently changes between years. We developed a workflow that takes these challenges into account (Fig. 7) (Rieger 2024, Rieger et al. 2025). First, we derive a routine that allows informed decisions about the most appropriate combination of residual families (Poisson or negative binomial), model covariates (e.g., habitat characteristics), and zero-inflation formulations to reflect species-specific data distributions. Second, we develop a correction factor that buffers population trend estimates for variation in observer expertise. Third, we integrate landscape-specific trends that adjust for between-year variation in the representation of habitat or landscape types within the yearly subset of sampled sites. Finally, by using generalized additive mixed models, we account for missing values due to rolling surveys. With these corrections in place, we find – within limits of the comparison – good consistency between the EAS trends and trends from the standard German common Bird monitoring scheme.

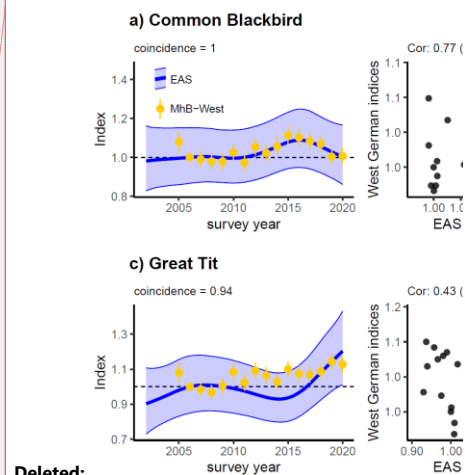


**Figure 7:** Trend comparison of EAS monitoring programme and West German MhB for four species. Left (per panel): Median Symmetric Accuracy (MSA) based on annual comparisons of indices. Right (per panel): correlation and correlation coefficients ( $\pm$  95% CI) of annual indices from 2005 to 2020. Both approaches exclude the baseline year 2006.

Deleted: 7  
Deleted: Coincidence of mean  
Deleted:  $\pm$  95% CrI (EAS) or CI (MhB-West).  
Deleted: - 2020  
Deleted: 34  
Deleted: 85  
Deleted: 62  
Deleted: 85  
Deleted: 8) (Rieger 2024, Rieger et al. 2024).  
Deleted: model weights

Challenges	Solutions
zero-inflation & overdispersion	<b>species-specific model optimization:</b> → <b>overdispersion:</b> nb, zinb → <b>zero-inflation</b> (including optimal covariate combination): zip, zinb nb = negative binomial, zinb = zero-inflated neg. binomial, zip = zero-inflated Poisson
observer effects (varying with time)	assess <b>observer effects</b> using: $\frac{\text{total abundance per site and year}^*}{\text{mean total abundance per site}^*}$ → <i>negative</i> (< 0.75), <i>none</i> (0.75-1.25), <i>positive</i> (>1.25) *summed up across all species
spatial bias (non-representative habitat coverage)	<b>smoothed trends per habitat</b> → <b>weighted posterior predictions</b> according to habitat share
rolling surveys (many missing values)	<b>generalized additive mixed models (GAMMs):</b> → smoothing function ( <i>additive</i> )* → site ID as random intercept ( <i>mixed</i> ) *based on thin plate regression splines

Figure 7: Workflow to address several challenges that arise when analysing breeding bird trends

Challenges	
zero-inflation & overdispersion	<b>species-s</b> → <b>overdi</b> → <b>zero-i</b> nb = neg; inflated F
observer effects (varying with time)	assess <b>ob</b> → <i>negat</i> *summer
spatial bias (non-representative habitat coverage)	<b>weighted</b> → <i>prever</i> composit
rolling surveys (many missing values)	<b>generaliz</b> → <i>smoo</i> → site ID *based o

Deleted:

Deleted: 8

#### 4.1 Distribution characteristics: Species specific optimisation

We found substantial variation in model structures that best reflected the empirical abundance distributions and fraction of structural zeros across the 61 study species. Model formulations spanned from simple Poisson or negative binomial models (e.g., European Green Woodpecker, Eurasian Blue Tit; 26.2 % of all modelled species) to models with elaborate zero inflation formulae to account for variation in the fraction of structural zeros across landscapes, study sites, or environmental covariates (e.g., Great Spotted Woodpecker or Willow Tit; 73.8 % of all modelled species, tab. 1). This variation often tied in with breeding ecologies (cf. examples in section 3.1). Widespread and abundant species with intermediate territory counts in many study sites typically required rather simple count models but no correction for structural zeroes. In contrast, heterogeneously distributed species with a high fraction of unoccupied sites or colonial breeders with often large territory numbers at the few occupied sites almost exclusively required the integration of zero inflation formulae, possibly connected with controls for variation in zero frequencies between regions, sites or environments. This diversity in distribution and abundance patterns is typical for most (bird) monitoring programmes independent of the chosen

Deleted:

Deleted: 85

Deleted: Common Kestrel and Blackbird; 27.1

Deleted: biogeographic regions

Deleted: Marsh

Deleted: 72.9

modelling approach, with similar choices documented elsewhere (Ettersson et al. 2009, Tirozzi et al. 2021, 2022, Hernández-Navarro et al. 2023).

#### 4.2 Spatial bias

Modelling trends per landscape type is an effective tool to avoid distorted trends due to spatial bias. This was exemplified by species such as Black Redstart, Eurasian Magpie, and Eurasian Nuthatch, showing striking diverging trends between metropolitan areas and other landscapes (Fig. 2, 4), which would otherwise bias regional or overall trends if discrepancies between landscape shares would be ignored. Similar distortions of trends or species distributions due to spatial bias often occur when using citizen science data since the sampled sites are selected by the observer and thus biased by its preferences (e.g., urban sites, sites of ecological interest (Johnston et al. 2020, Bowler et al. 2022))

Monitoring schemes should obviously aim to avoid the extreme disbalance in sampling that characterizes the early phase of the EAS monitoring, where each year focused on a subset of landscape types. Such bias is difficult to correct *a posteriori* and bears the risk that compensating for missing values leads to a high level of uncertainty, masking possible trends. However, when the yearly sampling subsets are representative and include all present landscapes, as in the EAS programme since 2013 (Fig. 2), our approach can unfold its full capacity by accounting for minor bias in habitat coverage or the overrepresentation of metropolitan areas among study sites.

#### 4.3 Observer effects

Observer effects caused substantial shifts in abundance estimates compared to West German breeding bird trends. The unfavourable combination of negative observer effects in early years of the EAS programme and positive effects in recent introduced a systematic shift towards more positive trends compared to MhB trends unless observer effects were considered. In severe cases, adding observer effects as covariate successfully buffered, as confirmed by comparison with West German breeding bird trends from the MhB programme of the DDA (Appendix section 4).

Our approach to categorize observer effects from site-specific abundance data risks to mask drastic increases or declines in true bird abundance, e.g., after a substantial change in habitat quality or land-use. Such extreme shifts, however, will typically have diverging species-specific effects on abundance with winners and losers (Lemoine et al. 2007), and thus appears unlikely to massively affect total abundance across species. Moreover, steady increases or declines in total abundance with habitat quality will also change mean total abundance across survey years, so that the threshold beyond which survey years are flagged as 'extreme' (positive or negative) also increases or decreases accordingly. Our

**Deleted:** We found more realistic EAS trend estimates after adding weights that reflect the degree of spatial bias among natural regions and metropolitan areas per year. This was exemplified by woodland species such as Chiffchaff, Chaffinch or Willow Warbler, which showed striking dips in uncorrected abundance estimates in 2006 where survey sites focused on agricultural landscapes with low woodland cover (Fig. 2). Weighting successfully buffered against yearly variation in the coverage of landscape types and thus provided more plausible trend estimates....

**Deleted:** weights for rare habitat types overly emphasise few surveys with exceptionally high or low population densities....

**Deleted:** weighting

**Deleted:** municipalities

**Deleted:** bias

**Deleted:** an overestimation of

**Deleted:** 6

**Deleted:** changes

1460 categorization fails, however, to identify cases of species-specific observer effects, such as insufficient  
expertise in discriminating ‘difficult’ species (e.g., songs of Garden Warbler vs. Blackcap) since total  
abundance is not affected by this, or hearing impairment for high pitched vocalisations (e.g., Goldcrest  
and Firecrest). For EAS, such cases are marked as implausible via an internal validating process and  
excluded from analysis (see section 2.5 ‘Data exclusion’).

Deleted: ),

1465 Alternative indices may capture components of observer effort beyond our rather simplistic  
representation of expertise. A widespread approach integrates survey duration or transect length as  
model covariates, or combines both measures into survey duration per unit length (Kéry et al. 2005).  
Kéry et al. (2005) found higher survey effort to increase the detection rates of many bird species,  
resulting in higher abundance estimates. Others integrated observer age as a (quadratic) model  
1470 covariate to correct for age-related changes in survey completeness (Farmer et al. 2014). Citizen Science  
data, e.g. those reported through online platforms such as ornitho (<https://www.ornitho.de/>) or ebird  
(<https://ebird.org/>), further allow estimating observer- and species-specific detection rates from species  
checklists, providing even more precise correction factors (Johnston et al. 2018). So far, the EAS  
monitoring programme did not provide data required to extract any of these covariates (i.e., effort, age,  
1475 detection rates), but we highly recommend their assessment to correct for possible observer effects.

Deleted: (Kéry et al. 2005, Kéry and Royle 2020).

Deleted: ,

Some of the observer effects inherent to the EAS dataset likely arise from individual differences in the  
approach to delineate breeding territories. In future refinements of the program, this could be mitigated  
by using point observations per survey instead of territories as the basis for trend analyses, possibly in  
hierarchical models comparable to those used in other monitoring programmes, e.g., the Swiss Breeding  
1480 Bird survey (Kéry et al. 2005, Strebel et al. 2020). Alternatively, territory delineation could be automated  
from raw point observations, e.g., using the AutoTerri algorithm from TerriMap online developed by the  
Swiss Ornithological Institute (Wechsler 2018).

Deleted: (Kéry et al. 2005, Kéry and Royle 2020, Strebel et al. 2020)...

#### 4.4 Consistency check

1485 Population trend estimates for 59 species revealed a reasonably close match between the GAMM-based  
trend smoothers applied on the EAS dataset and TRIM-based yearly point estimates applied in the West  
German common breeding bird census. Despite substantial differences in the chosen modelling  
approach and spatial coverage, most trend estimates had solid positive correlations and/or a good  
Median Symmetric Accuracy between annual indices (Fig. 6, Appendix section 5). In many cases,  
1490 smoothed GAMM-trends for the EAS data captured even short-term population fluctuations at a 3–7-  
year scale, similar to the – by definition – more fine-grained yearly MhB indices (e.g., Common Blackbird,  
Eurasian Wren, Firecrest, Appendix section 5). Neutral or even negative correlations between yearly  
EAS- and MhB-indices occurred primarily in two species subsets. The first concerns colonial birds (e.g.,

Deleted: coincidence

Deleted: 7

Deleted: 7

Deleted: 7



Common Swift, [Eurasian](#) Tree Sparrow, Common House Martin, Barn Swallow, Appendix section [5](#)) where trend estimates are highly sensitive to the share of study sites with colonies present, the influence of few large colonies on the trend estimates, the precision of nest counts, and observer access to a given colony (Südbeck et al. 2005, LANUV 2016a). The second subset concerns species with pronounced affinity to urban areas as derived from low or high coefficient estimates for the linear effect of PC3 (Appendix section [6](#)), where affinity can be positive (e.g., Eurasian Magpie, Dunnock, Common House Martin, Common Kestrel and Black Redstart) or negative (e.g., Common Chaffinch, Eurasian Jay, Marsh Tit or Crested Tit). Given an exceptionally high share and density of urban areas in NRW compared to other West German federal states, NRW trends are plausibly more positive than West German MhB trends for urban specialists (e.g., Eurasian Magpie, Dunnock, Common Kestrel, Black Redstart, Appendix section [5](#)) and more negative for non-urban species (e.g. Common Chaffinch and Crested Tit, Appendix section [5](#)).

Deleted: 7

Deleted: 8

Deleted: 7

Deleted: 7

## 5 Conclusion

We developed a modelling routine for bird population trend analyses that [can handle](#) several common [problems in monitoring data](#). Our approach accounts for unbalanced sampling of landscape types, optimises species-specific model structure with respect to zero-inflation and overdispersion, partially accounts for variation in observer expertise, and integrates GAM-based smoothing to bridge even extensive gaps between replicated surveys in a ‘rolling’ sampling design. Our consistency check against trends from the Germany common breeding bird programme indicates that our routine produces reliable and robust trends for most species. The R script and package provided with this study can be adapted to other monitoring programmes with comparable survey designs and data structures.

Deleted: avoids

Deleted: weaknesses

Deleted: existing approaches

## Acknowledgements

We thank the many observers for contributing to the EAS and MhB monitoring programmes, Matteo Santon for statistical and computational advice, and Jakob Katzenberger, Johannes Kamp, and Johannes Wahl for comments on earlier versions of this workflow. [We also thank Matthieu Paquet and two anonymous referees for their helpful feedback during the submission process.](#)

## Funding

The development of this workflow has been financially supported by State Agency for Nature, Environment and Consumer Protection in North Rhine-Westphalia (LANUV) to University of Tübingen.

#### Conflict of interest disclosure

The authors declare that they comply with the PCI rule of having no financial conflicts of interest in relation to the content of the article.

#### Data, scripts, code and supplementary information availability

A data example for five species, R script, and code are available from Github ([https://github.com/m-rieger/EAS\\_bird](https://github.com/m-rieger/EAS_bird)) (Rieger et al. 2025) as well as a package with helper functions (<https://github.com/m-rieger/EAS>) (Rieger 2024). Further figures, model outputs and detailed descriptions are provided in the electronic supplementary material ('EAS-bird\_Appendix.html').

**Deleted:** (Rieger et al. 2024)

## References

- 1555 ATKIS. 2013. Amtliches Topographisch-Kartographisches Informationssystem. <https://www.adv-online.de/Adv-Produkte/Geotopographie/ATKIS/>
- Blasco-Moreno, A., M. Pérez-Casany, P. Puig, M. Morante, and E. Castells. 2019. What does a zero mean? Understanding false, random and structural zeros in ecology. *Methods in Ecology and Evolution* **10**: 949-959. <https://doi.org/10.1111/2041-210X.13185>
- 1560 Bogaart, P., M. van der Loo, and J. Pannekoek. 2020. Package 'rtrim' - Trends and Indices for Monitoring Data, version 2.1.1. R package. <https://github.com/markvanderloo/rtrim>
- Bowler, D. E., C. T. Callaghan, N. Bhandari, K. Henle, M. Benjamin Barth, C. Koppitz, R. Klenke, M. Winter, F. Jansen, and H. Bruelheide. 2022. Temporal trends in the spatial bias of species occurrence records. *Ecography* **2022**: e06219. <https://doi.org/10.1111/ecog.06219>
- 1565 Buckland, S., and A. Johnston. 2017. Monitoring the biodiversity of regions: Key principles and possible pitfalls. *Biological Conservation* **214**: 23-34. <https://doi.org/10.1016/j.biocon.2017.07.034>
- Bürkner, P.-C. 2017. brms: An R package for Bayesian multilevel models using Stan. *Journal of statistical software* **80**: 1-28. <https://doi.org/10.18637/jss.v080.i01>
- 1570 Burns, F., M. A. Eaton, I. J. Burfield, A. Klvaňová, E. Šilarová, A. Staneva, and R. Gregory. 2021a. Abundance decline in the avifauna of the European Union conceals complex patterns of biodiversity change. *Authorea Preprints*. <https://doi.org/10.22541/au.162557488.83915072/v1>
- Burns, F., M. A. Eaton, I. J. Burfield, A. Klvaňová, E. Šilarová, A. Staneva, and R. D. Gregory. 2021b. Abundance decline in the avifauna of the European Union reveals cross-continental similarities in biodiversity change. *Ecology and Evolution* **11**: 16647-16660. <https://doi.org/10.1002/ece3.8282>
- 1575 Campbell, H. 2021. The consequences of checking for zero-inflation and overdispersion in the analysis of count data. *Methods in Ecology and Evolution* **12**: 665-680. <https://doi.org/10.1111/2041-210X.13559>
- 1580 CDC. 2010. Deutscher Wetterdienst Climate Data Center: Vieljährige Stationsmittelwerte für die Klimareferenzperiode 1981-2010. [https://www.dwd.de/DE/klimaumwelt/cdc/cdc\\_node.html](https://www.dwd.de/DE/klimaumwelt/cdc/cdc_node.html)
- Dakki, M., G. Robin, M. Suet, A. Qninba, M. A. El Agbani, A. Ouassou, R. El Hamoumi, H. Azafzaf, S. Rebah, and C. Feltrup-Azafzaf. 2021. Imputation of incomplete large-scale monitoring count data via penalized estimation. *Methods in Ecology and Evolution* **12**: 1031-1039. <https://doi.org/10.1111/2041-210X.13594>
- 1585 Etterson, M. A., G. J. Niemi, and N. P. Danz. 2009. Estimating the effects of detection heterogeneity and overdispersion on trends estimated from avian point counts. *Ecological applications* **19**: 2049-2066. <https://doi.org/10.1890/08-1317.1>
- 1590 Farmer, R. G., M. L. Leonard, J. E. Mills Flemming, and S. C. Anderson. 2014. Observer aging and long-term avian survey data quality. *Ecology and Evolution* **4**: 2563-2576. <https://doi.org/10.1002/ece3.1101>
- Fewster, R. M., S. T. Buckland, G. M. Siriwardena, S. R. Baillie, and J. D. Wilson. 2000. Analysis of population trends for farmland birds using generalized additive models. *Ecology* **81**: 1970-1984. [https://doi.org/10.1890/0012-9658\(2000\)081\[1970:AOPTF2\]2.0.CO;2](https://doi.org/10.1890/0012-9658(2000)081[1970:AOPTF2]2.0.CO;2)
- 1595 Gabry, J., and R. Češnovar. 2020. Cmdstanr: R interface to 'CmdStan'. <https://github.com/stan-dev/cmdstanr/>
- Hernández-Navarro, A. J., F. Robledano, M. V. Jiménez-Franco, J. A. Royle, and J. F. Calvo. 2023. Long-term trends of local bird populations based on monitoring schemes: are they suitable for justifying management measures? *Journal of Ornithology*: 1-13. <https://doi.org/10.1007/s10336-023-02114-3>
- 1600 Jennings, K. 2021. Deploying data for nature conservation: How monitoring data is used to inform conservation policy and practice [Keynote address]. BOUsci21 - Developments in monitoring science, United Kingdom, November 24-25.

- 1605 Jiguet, F. 2009. Method learning caused a first-time observer effect in a newly started breeding bird survey. *Bird Study* **56**: 253-258. <https://doi.org/10.1080/00063650902791991>
- Jiguet, F., M. Barbet-Massin, V. Devictor, N. Jonzén, and Å. Lindström. 2013. Current population trends mirror forecasted changes in climatic suitability for Swedish breeding birds. *Bird Study* **60**: 60-66. <https://doi.org/10.1080/00063657.2012.733337>
- 1610 Johnston, A., D. Fink, W. M. Hochachka, and S. Kelling. 2018. Estimates of observer expertise improve species distributions from citizen science data. *Methods in Ecology and Evolution* **9**: 88-97. <https://doi.org/10.1111/2041-210X.12838>
- Johnston, A., D. Fink, M. D. Reynolds, W. M. Hochachka, B. L. Sullivan, N. E. Bruns, E. Hallstein, M. S. Merrifield, S. Matsumoto, and S. Kelling. 2015. Abundance models improve spatial and temporal prioritization of conservation resources. *Ecological applications* **25**: 1749-1756. <https://doi.org/10.1890/14-1826.1>
- 1615 Johnston, A., N. Moran, A. Musgrove, D. Fink, and S. R. Baillie. 2020. Estimating species distributions from spatially biased citizen science data. *Ecological Modelling* **422**: 108927. <https://doi.org/10.1016/j.ecolmodel.2019.108927>
- 1620 Kamp, J., C. Frank, S. Trautmann, M. Busch, R. Dröschmeister, M. Flade, B. Gerlach, J. Karthäuser, F. Kunz, and A. Mitschke. 2021. Population trends of common breeding birds in Germany 1990–2018. *Journal of Ornithology* **162**: 1-15. <https://doi.org/10.1007/s10336-020-01830-4>
- Kéry, M., J. A. Royle, and H. Schmid. 2005. Modeling avian abundance from replicated counts using binomial mixture models. *Ecological applications* **15**: 1450-1461. <https://doi.org/10.1890/04-1120>
- 1625 Klvaňová, A., P. Voříšek, R. D. Gregory, A. van Strien, and A. Gmelig Meyling. 2009. Wild birds as indicators in Europe: latest results from the Pan-European Common Bird Monitoring Scheme (PECBMS). *Avocetta* **33**: 7-12.
- Knappe, J. 2016. Decomposing trends in Swedish bird populations using generalized additive mixed models. *Journal of Applied Ecology* **53**: 1852-1861. <https://doi.org/10.1111/1365-2664.12720>
- 1630 König, H. 2020. Standards und Indikatorartengruppen - Erfahrungen aus der ÖFS in Nordrhein-Westfalen. Pages 17-32 in W. Züghart, S. Stenzel, and B. Fritsche, editors. *Umfassendes bundesweites Biodiversitätsmonitoring*. BfN Schriften. <https://www.bfn.de/sites/default/files/BfN/service/Dokumente/skripten/skript585.pdf>
- 1635 Korner-Nievergelt, F., T. Roth, S. Von Felten, J. Guélat, B. Almasi, and P. Korner-Nievergelt. 2015. Bayesian data analysis in ecology using linear models with R, BUGS, and Stan. Academic Press. <https://doi.org/10.1016/C2013-0-23227-X>
- LANUV. 2016a. Arbeitsanleitung für Brutvogel-Revierkartierungen im Auftrag des LANUV NRW. Landesamt für Natur, Umwelt und Verbraucherschutz Nordrhein-Westfalen, Recklinghausen, Germany: 1-79. [https://methoden.naturschutzinformationen.nrw.de/methoden/web/babel/media/Arbeitsanleitung\\_fuer\\_Brutvogel\\_Revierkartierungen\\_NRW.pdf](https://methoden.naturschutzinformationen.nrw.de/methoden/web/babel/media/Arbeitsanleitung_fuer_Brutvogel_Revierkartierungen_NRW.pdf)
- 1640 LANUV. 2016b. Daten zu Natur in Nordrhein-Westfalen 2016 - LANUV-Fachbericht 83. Landesamt für Natur, Umwelt und Verbraucherschutz Nordrhein-Westfalen, Recklinghausen, Germany: 1-216. [https://www.lanuv.nrw.de/fileadmin/lanuvpubl/3\\_fachberichte/Daten\\_zur\\_Natur\\_in\\_NRW\\_2016.pdf](https://www.lanuv.nrw.de/fileadmin/lanuvpubl/3_fachberichte/Daten_zur_Natur_in_NRW_2016.pdf)
- 1645 Lemoine, N., H.-G. Bauer, M. Peintinger, and K. Böhning-Gaese. 2007. Effects of climate and land-use change on species abundance in a central European bird community. *Conservation Biology* **21**: 495-503. <https://doi.org/10.1111/j.1523-1739.2006.00633.x>
- 1650 Link, W. A., and J. R. Sauer. 1998. Estimating population change from count data: application to the North American Breeding Bird Survey. *Ecological applications* **8**: 258-268. [https://doi.org/10.1890/1051-0761\(1998\)008\[0258:EPCFCD\]2.0.CO;2](https://doi.org/10.1890/1051-0761(1998)008[0258:EPCFCD]2.0.CO;2)
- 1655 Morley, S. K., T. V. Brito, and D. T. Welling. 2018. Measures of model performance based on the log accuracy ratio. *Space Weather* **16**: 69-88.

Niemelä, J. 2000. Biodiversity monitoring for decision-making. Pages 307-317 in *Annales Zoologici Fennici*. JSTOR. <http://www.jstor.org/stable/23735723>

1660 Pannekoek, J., and A. J. van Strien. 2001. TRIM 3 manual (Trends & Indices for Monitoring Data). CBS Statistics Netherlands, Voorburg, The Netherlands.

Pöysä, H., J. Rintala, A. Lehtikainen, and R. A. Väisänen. 2013. The importance of hunting pressure, habitat preference and life history for population trends of breeding waterbirds in Finland. *European Journal of Wildlife Research* **59**: 245-256. <https://doi.org/10.1007/s10344-012-0673-8>

1665 R Core Team. 2024. R: a language and environment for statistical computing. R Foundation for Statistical Computing website. <https://www.R-project.org/>

Ribeiro Jr, P. J., and P. J. Diggle. 2020. Package 'geoR' - Analysis of Geostatistical Data. R package. <http://www.leg.ufpr.br/geoR/>

1670 Rieger, M. R. 2024. EAS - Module to analyse population trends from monitoring data with highly structured sampling designs. Zenodo. <https://doi.org/10.5281/zenodo.12517388>

Rieger, M. R., C. Grüneberg, M. Oberhaus, S. Trautmann, M. Parepa, and N. Anthes. 2025. EAS\_bird - Data and script of 'Bird population trend analyses for a monitoring scheme with a highly structured sampling design'. Zenodo. <https://doi.org/10.5281/zenodo.12518872>

1675 Sauer, J. R., K. L. Pardieck, D. J. Ziolkowski Jr, A. C. Smith, M.-A. R. Hudson, V. Rodriguez, H. Berlanga, D. K. Niven, and W. A. Link. 2017. The first 50 years of the North American breeding bird survey. *The Condor: Ornithological Applications* **119**: 576-593. <https://doi.org/10.1650/CONDOR-17-83.1>

Sauer, J. R., B. G. Peterjohn, and W. A. Link. 1994. Observer differences in the North American breeding bird survey. *The Auk* **111**: 50-62. <https://doi.org/10.2307/4088504>

1680 Strebel, N., R. Dröschmeister, H. Schmid, I. Stützel, S. Trautmann, and J. Wahl. 2020. Ein Vergleich zwischen revier- und individuenbasierten Verfahren zum Abschätzen von Brutbestandsindizes im Monitoring häufiger Brutvögel. *Die Vogelwelt* **140**: 183-206.

Südbeck, P., H. Andretzke, K. Gedeon, T. Schikore, K. Schröder, S. Fischer, and C. Sudfeldt. 2005. Methodenstandards zur Erfassung der Brutvögel Deutschlands. Max-Planck-Institut für Ornithologie. Vogelwarte Radolfzell.

1685 Tirozzi, P., V. Orioli, O. Dondina, L. Kataoka, and L. Bani. 2021. Species Traits Drive Long-Term Population Trends of Common Breeding Birds in Northern Italy. *Animals* **11**: 3426. <https://doi.org/10.3390/ani11123426>

Tirozzi, P., V. Orioli, O. Dondina, L. Kataoka, and L. Bani. 2022. Population trends from count data: handling environmental bias, overdispersion and excess of zeroes. *Ecological Informatics* **69**: 101629. <https://doi.org/10.1016/j.ecoinf.2022.101629>

1690 van Strien, A., J. Pannekoek, W. Hagemeijer, and T. Verstrael. 2004. A loglinear Poisson regression method to analyse bird monitoring data. *Bird* **482**: 33-39. <https://api.semanticscholar.org/CorpusID:15188304>

1695 van Strien, A. J., J. Pannekoek, and D. W. Gibbons. 2001. Indexing European bird population trends using results of national monitoring schemes: a trial of a new method. *Bird Study* **48**: 200-213. <https://doi.org/10.1080/00063650109461219>

Vorisek, P., R. D. Gregory, A. J. Van Strien, and A. G. Meyling. 2008. Population trends of 48 common terrestrial bird species in Europe: results from the Pan-European Common Bird Monitoring Scheme. *Revista Catalana d'Ornitologia* **24**: 4-14. <https://pecbms.info/wp-content/uploads/2022/01/vorisek-et-al-2008.pdf>

1700 Wechsler, S. 2018. Automating the analysis of territory mapping data in bird monitoring. UNOGIS-Paris Lodron-Universität Salzburg. <https://api.semanticscholar.org/CorpusID:53652000>

Weiss, J., and K. Schulze-Hagen. 2014. Viele Menschen—viele Vögel? Ornithologie und Vogelschutz in Nordrhein-Westfalen. *Charadrius* **50**: 3-22.

1705 Wood, S. 2021. mgcv - Mixed GAM Computation Vehicle with Automatic Smoothness Estimation. R package: 1-323. <https://doi.org/10.32614/CRAN.package.mgcv>

1710

Zuur, A. F. 2012. A beginner's guide to generalized additive models with R. Highland Statistics Limited  
Newburgh, NY, USA.

Deleted: ¶  
¶